# The Phase Response Values Application of Second-Order Digital Frequency-Dependent Components for Calculating Transfer Function Coefficients in Robotic Systems

Hanna Ukhina[0000-0003-3797-1460], Ivan Afanasyev[0000-0002-3207-5741X], Valerii Sytnikov[0000-0003-3229-5096], Oleg Streltsov[0000-0002-4691-5703], Pavel Stupen[0000-0003-1952-6144]

Odessa National Polytechnic University, Odessa, Ukraine
ukhinanna@gmail.com, nekaktotak2@gmail.com, sitnvs@gmail.com, ovstreltsov@gmail.com, stek2000@gmail.com

**Abstract.** This study deals with the influence of the second order tunable digital frequency-dependent components' transfer function coefficients on the phase response during those components tuning. The obtained approximations of phase frequency responce dependence on the ripple level allowed us to find the digital filter transfer function of the denominator coefficients values. It is worth noting that this expression works at ripple level up to 40 with a standard error of 0,06% for Chebyshev filter-1 and 0.28% for Chebyshev filter-2. Also in these work we fix the ripple level. With this value, for each cutoff level and ripple level we determine the phase value and to obtain the three-dimensional graph approximation. Theoretical studies have been verified experimentally

**Keywords:** Industry 4.0, Internet of Things, Robotic Platforms, Frequency Characteristics

## 1 Introduction

At modern epoque the development of information management systems and robotic systems takes place in accordance with the Industry 4.0 concept. In the framework of this direction, there is a need to improve existing and develop new approaches to the components development of such systems with the criteria of mobility, flexibility, the ability to quickly restructure and adaptability to their operating conditions [1].

Exiting of the Internet of things (IoT) technology implies the information exchange not only between people and "things", but also between "things", i.e. computerized machines, devices, components, and sensors.

On the one hand, "things" equipped with sensors can exchange data and process information without human engaging to that process, and on the other hand, a human

can actively participate in the process, for example, when it comes to "smart devices" or "smart enterprise " concepts.

A smart enterprise is a subcategory of IoT, embodying as its kind, the industrial Internet of things (IIoT). Therefore, today the technological equipment and facilities components are equipped with multifunctional sensors, actuators and controllers.

Using of Internet technologies and wireless networks to them facilitates the data rapid collection, their primary processing and presentation to the operator in a convenient form for prompt and timely decision-making. However, increasing the automation level in all areas of the enterprise allows you to organize production without the people participation. In this regard, robotic industries are in the first place, as are robotic platforms.

The personnel role in this case is reduced to the control of the technological process and response to emergency situations [1-6]. This task is especially acute for robotic platforms and critical application systems that must operate in difficult conditions without human access [7-10].

Then, there arises a problem of building the robotic computer systems capable for a comprehensive rearrangement of their characteristics by soft- and hardware tools, depending on the operating conditions to increase the system efficiency is relevant. It should be noted that the signal processing path of such systems uses frequency-dependent components (FDC), representing a combination of hard- and software arranged in a complex architecture and including a variety of linkages [11-14].

Well-known is that the FDC responses do uniquely depend on the transfer function coefficients [7].

Then, while calculating the coefficients, we can take into account the peculiar characteristics of both the amplitude-frequency response (AFR) and phase-frequency (PFR) response.

Let's consider the influence of the second order tunable digital frequency-dependent components' phase-frequency response values when a smooth amplitude-frequency response while calculating the transfer function coefficients [15].

## 2 The influence of the frequency-dependent components transfer function coefficients on the its characteristics

Here we shall consider the widely used typical digital filters as a component of signal processing and filtering path. Well known is that for ease of tuning the high-order components are built on the basis of first and second orders frequency-dependent components (FDC) [7].

Therefore, the analysis of the digital filter transfer function coefficients' influence on the digital filter responses properties is carried out using the second-order transfer function, which has the form

$$H(z) = \frac{a_0 + a_1 z^{-1} + a_2 z^{-2}}{1 + b_1 z^{-1} + b_2 z^{-2}} \quad (1)$$

where $a_0, a_1, a_2, b_1, b_2$ are the real coefficients of the numerator and denominator. When substituting $z^{-1} = e^{-j\varpi}$ or using Euler's formula $z^{-1} = \cos(\varpi) - j\sin(\varpi)$, where $\varpi$ is the normalized angular frequency, $\varpi = \frac{2\pi \frac{f}{f_d}}{\pi}$, $\varpi \in [0, \pi]$, $f$, $f_d$ are the linear frequency and the sampling frequency, respectively, we get a complex transfer coefficient, and based on this coefficient, the amplitude-frequency response (AFR) and phase-frequency response (PFR): at $a_0 = -a_2$ [13]

$$H(\varpi) = \sqrt{a_0^2 \frac{2 + \left(\frac{a_1}{a_0}\right)^2 + 4\left(\frac{a_1}{a_0}\right)\cos(\varpi) + 2\cos(2\varpi)}{1 + b_1^2 + b_2^2 + 2b_1(1 + b_2)\cos(\varpi) + 2b_2\cos(2\varpi)}}, \quad (2)$$

$$\phi(\varpi) = arctg\left(\frac{(b_2 - 1)\sin(\omega)}{(b_2 + 1)\cos(\varpi) + b_1}\right) \quad (3)$$

It should be noted that similar equations are used to describe the digital filters, and typical second order links at automatic control systems. Therefore, we consider the influence of the transfer function coefficients onto the frequency response of second order low-pass (LP) digital filters, as the most used frequency-dependent component used at computer systems and control systems.

For polynomial filters, the relation $a_1 = 2a_0$, which makes it possible to get the amplitude frequency response square from the formula (2) upon certain transformations carried out

$$H^2(\varpi) = \frac{4a_0^2(1 + \cos(\varpi))^2}{(1 - b_2)^2 + (b_1 + 2\cos(2\varpi))(b_1 + 2b_2\cos(\varpi))} \quad (4)$$

From equation (3) for the Butterworth filter and with respect to PFR type (Fig.1), it can be specified that the phase value at cutoff frequency $\varphi(\varpi_c) = -\frac{\pi}{2}$. Then the PFR denominator will appear like

$$(b_2 + 1)\cos(\varpi) + b_1 = 0$$

We define $b_1$ as

$$b_1 = -(b_2 + 1)\cos(\varpi) \quad (5)$$

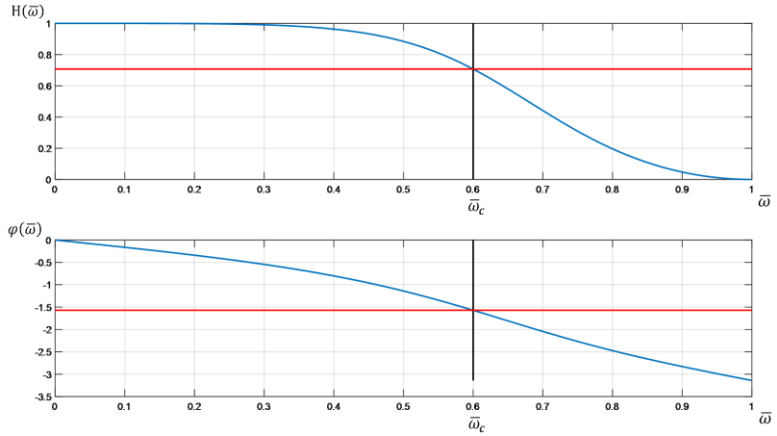


**Fig. 1.** Frequency and phase response of the second order Butterworth filter

For the Chebyshev filter-1, this solution is not possible, because here the PFR has different phase values at frequency the cutoff level $c$ set by the ripple value in the bandwidth $\varepsilon$ . It should be noted that in the most mathematical packages, the ripple level is set in RP decibels further recalculated to $c$ as follows

$$c = \frac{1}{\sqrt{10^{0.1RP}}}$$

For the Butterworth digital filter, the RP value is constantly -3 dB ($c = 0.707$), and for other filters it has different values, but the value $c$ is in the range $0 < c < 1$, refer to Fig. 2 and 3.

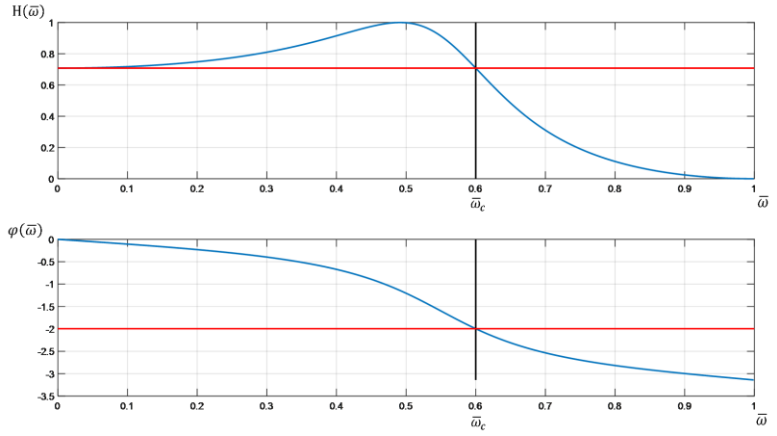


**Fig. 2.** Amplitude frequency response and frequency response of the second order Chebyshev filter-1 at RP= -3 dB

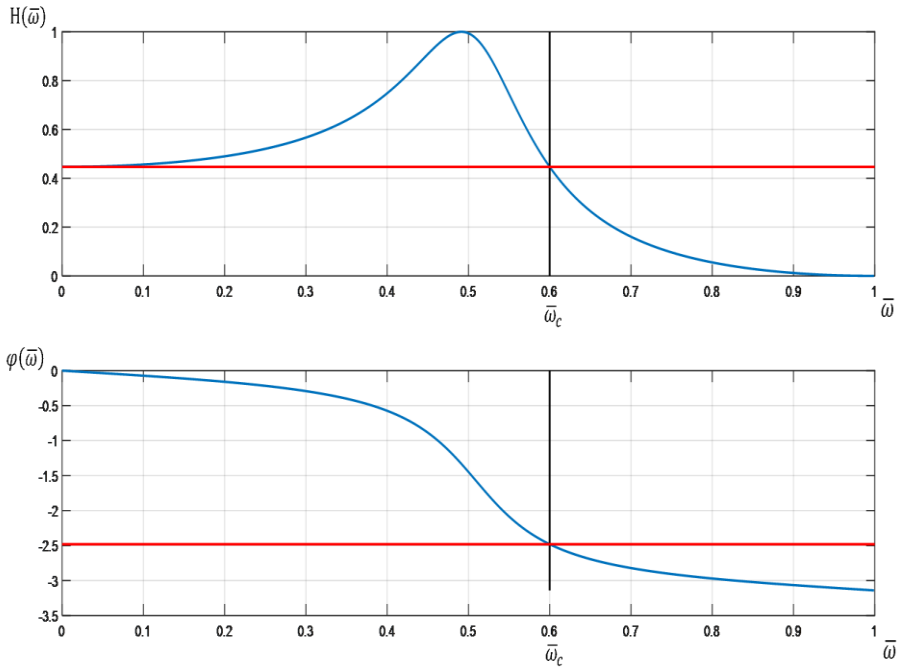


**Fig. 3.** Amplitude frequency response and frequency response of the second order Chebyshev filter -1, at RP= - 7dB

Studies of PFR have shown that one of its main features is not a dependence on the cutoff frequency, but the dependence on the ripple level. This phenomenon is manifested differently in different filters.

After all transformations based on equations (2) and (3), the coefficients $b_1$ and $b_2$ for the Chebyshev filter -1 will have the form

$$b_1 = -\left[\left(1+b_2\right)\cos\left(\varpi_c\right)+\frac{1-b_2}{\phi}\sin\left(\varpi_c\right)\right]$$

$$b_2 = \frac{\left[2\sqrt{1+\phi^2}+\left(1+\cos\left(\varpi_c\right)\right)\right]-\phi\sin\left(\varpi_c\right)}{\left[2\sqrt{1+\phi^2}+\left(1+\cos\left(\varpi_c\right)\right)\right]+\phi\sin\left(\varpi_c\right)}$$

where $\phi = tg\left(\varphi\right)$ from formula (3).

As evidently seen, to calculate the coefficients $b_1$ and $b_2$ it is necessary to know the cutoff frequency PFR values at different ripple level values in the bandwidth.

It follows from Figures 2 and 3 that the phase values at the cutoff frequency depend only on the ripple level in the bandwidth, Fig.4 [12].

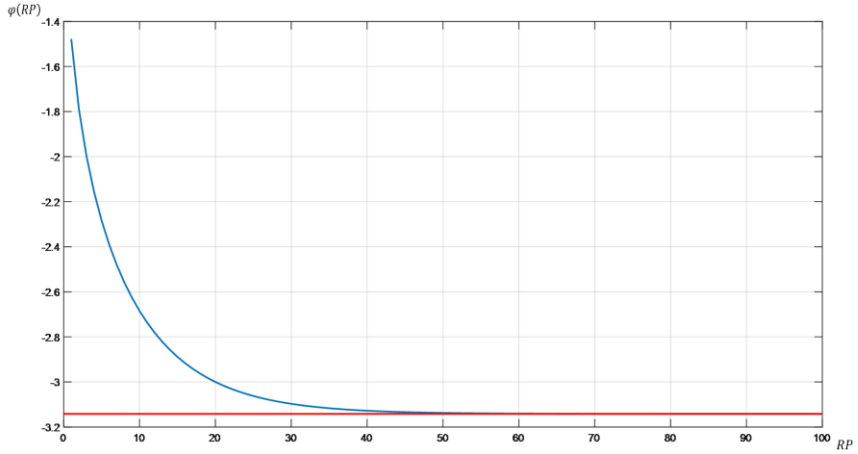


**Fig. 4.** Dependence of Chebyshev's LP-1 FDC PFR at cutoff frequency ω`=0.5 on the ripple level

To be noted is that if the ripple level is constant and the cutoff frequency varies, this value does never change. The approximation of this dependence has the form

$$\varphi = -\pi thx = -\pi\left[\frac{x\left[\left(1+0.1666x^2\right)+0.008x^4\left(1+0.0241x^2\right)\right]}{\left(1+0.5x^2\right)+0.0417x^4\left(1+0.0335x^2\right)}\right]$$

It is worth noting that this expression works at RP up to 40 with a standard error of 0,06%. The resulting transformation is shown in Figure 5.

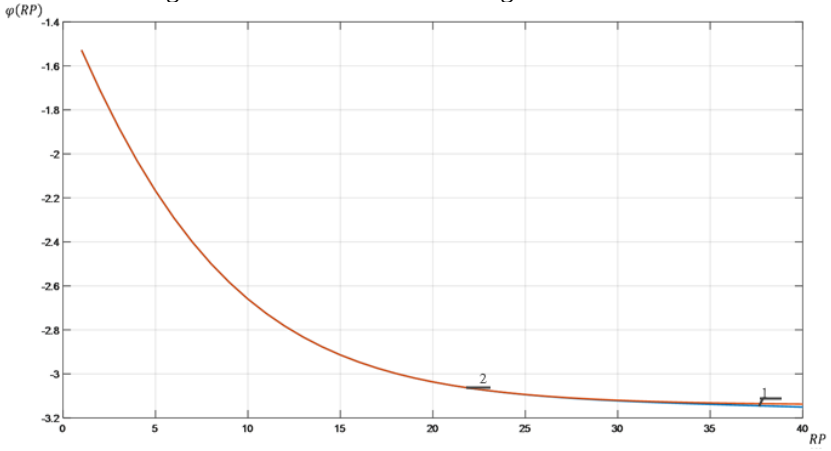


**Fig. 5.** Tabulated values (1) and approximating function (2) graphs

If we consider the Chebyshev filter-1 phase value as the limit value equal to -π, then the expansion into series allows using it only up to the bandwidth ripple level value equal to 35.

Applying this approach to finding the non-polynomial Chebyshev filter-2 coefficients has its own peculiarities. For the Chebyshev filter-2, this solution is not possible, because here the PFR has different phase values at the cutoff frequency level $cs$ set by the ripple value in the bandwidth $\varepsilon$. The ripple level is set in RP decibels further recalculated to $cs$ the same as $c$ in the most mathematical packages.

For the Chebyshev filter-2, the phase also has a different value depending on the $cs$ value, Fig. 6 and 7.

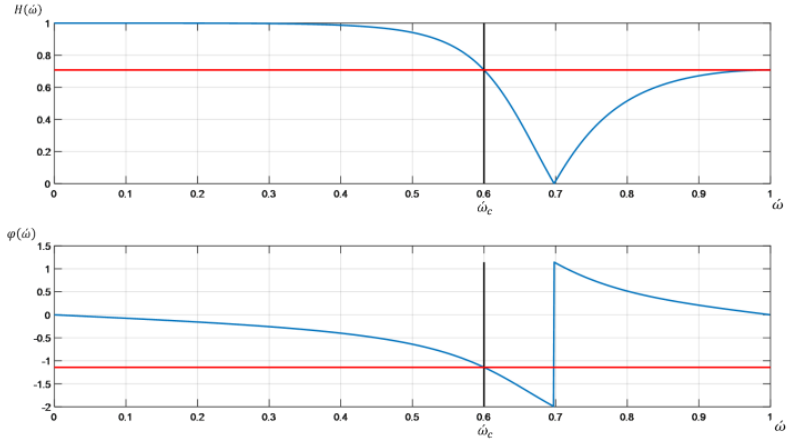


**Fig. 6.** Amplitude frequency response and phase frequency response of the second order Chebyshev filter-2 at RP= -3

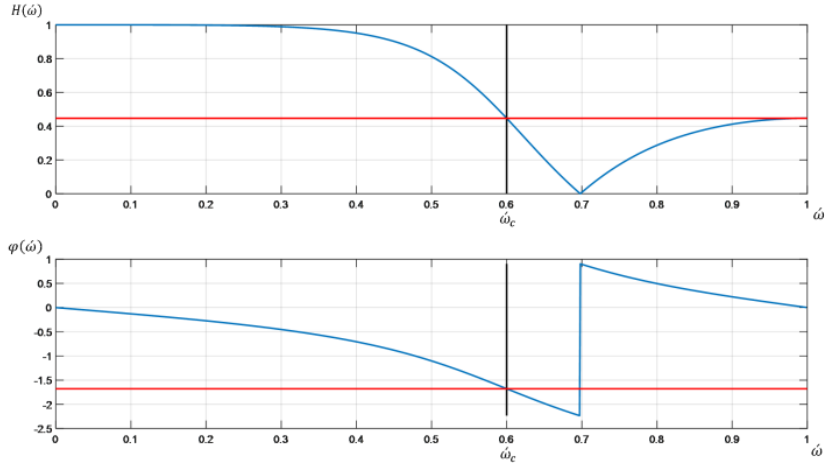


**Fig. 7.** Amplitude frequency response and phase frequency response of the second order Chebyshev filter-2, at RP= - 7dB

After all transformations based on equations (2) and (3), the coefficients $b_1$ and $b_2$ for the Chebyshev filter -2 will have the form

$$b_1 = -\frac{(1-b_2)\sin(\varpi_c)+(1+b_2)\phi\cos(\varpi_c)}{\phi}$$

$$b_2 = \frac{\left[2cs\sqrt{1+\phi^2}-(1+cs)-(1-cs)\cos(\varpi_c)\right]+\phi(1-cs)\sin(\varpi_c)}{\left[2cs\sqrt{1+\phi^2}-(1+cs)-(1-cs)\cos(\varpi_c)\right]-\phi(1-cs)\sin(\varpi_c)}$$

where $\phi = tg(\varphi)$ from formula (3).

As evidently seen, to calculate the coefficients $b_1$ and $b_2$ it is necessary to know the cutoff frequency PFR values at different ripple level values in the bandstop. If the ripple level is constant and the cutoff frequency varies, this value does never change. From figures 6 and 7 we can conclude that the phase values at the cutoff frequency depend only on the level of ripples in the bandstop, Fig. 8 [15].

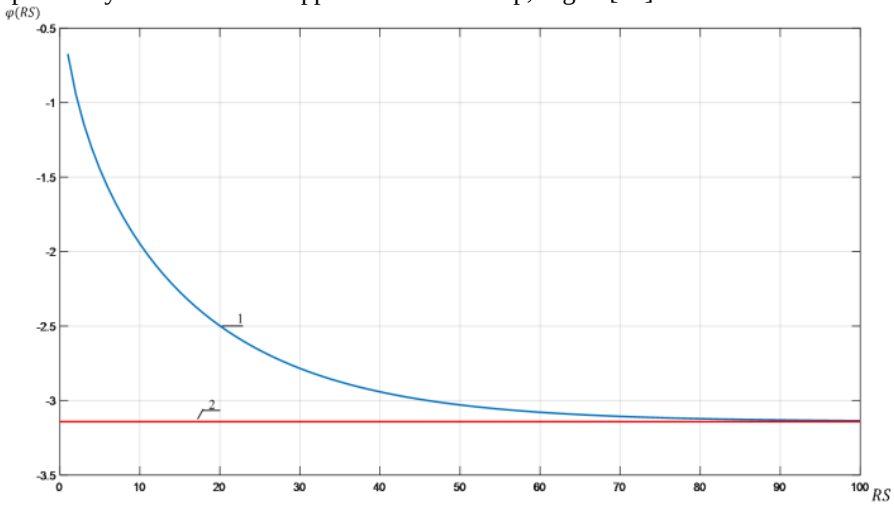


**Fig. 8.** Tabulated values (1) and approximating function (2) graphs

The first approximations gave us the dependence of the kind shown in Fig.9.

$$\varphi = -\pi thx = -\pi\left[\frac{x\left[\left(1+0.1666x^2\right)+0.008x^4\left(1+0.0241x^2\right)\right]}{\left(1+0.5x^2\right)+0.0417x^4\left(1+0.0335x^2\right)}\right]$$

The mean square error in this case is 0.28%.

Transitions to the non-polynomial Cauer filter (elliptic) after all transformations based on equations (2) and (3), the coefficients $b_1$ and $b_2$ will have the form

$$b_1 = -\frac{(1-b_2)\sin(\varpi_c)+(1+b_2)\phi\cos(\varpi_c)}{\phi}$$

$$b_2 = \frac{\left[2c\sqrt{1+\phi^2}+(c+cs)+(c-cs)\cos(\varpi_c)\right]-\phi(c-cs)\sin(\varpi_c)}{\left[2c\sqrt{1+\phi^2}+(c+cs)+(c-cs)\cos(\varpi_c)\right]+\phi(1-cs)\sin(\varpi_c)}$$

where $\phi = tg(\varphi)$ from formula (3).

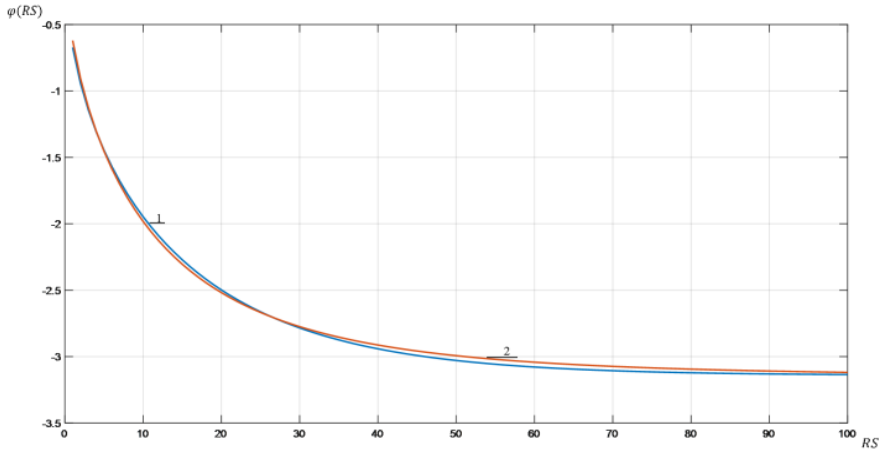


**Fig. 9.** Tabulated values (1) and approximating function (2) graphs

As evidently seen, to calculate the coefficients $b_1$ and $b_2$ it is necessary to know the cutoff frequency PFR values at different ripple level values $c$ and $cs$. If the ripple level is constant $c$ and $cs$, this value does never change, Fig. 10.

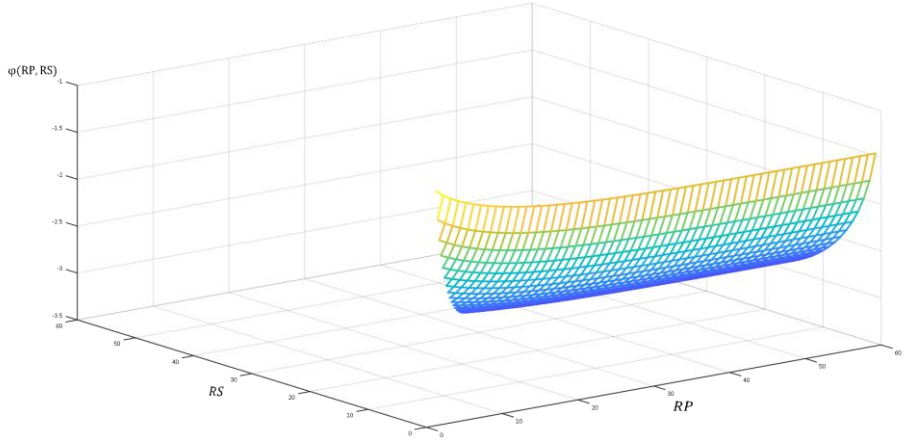


**Fig. 10.** Tabulated values graph

To obtain the three-dimensional graph approximation, we go the following way. We fix the ripple level $cs$ or RS.
With this value, for each $c$ or RP we determine the phase value. Thus, having drawn sections for a three-dimensional graph, Fig. 10, one can find the approximating function description $\varphi = f(RP)$, for a given RS. Such a function will be a quadratic equation and have the form

$$\varphi = -\pi\left(aRP^2 + bRP + c\right)$$

The coefficient values $a, b$ and $c$ have found for different RS values, table 1.

**Table 1.** The coefficient values a, b, and c for different RS values

| RS | a | b | c |
|---|---|---|---|
| 5 | -0.0097 | 0.1368 | 0.2685 |
| 7 | -0.0063 | 0.1236 | 0,3051 |
| 10 | -0,0040 | 0,1110 | 0,3489 |
| 15 | -0,0022 | 0,0986 | 0,4032 |
| 20 | -0,0015 | 0,0910 | 0,4421 |
| 30 | -0,0008 | 0,0820 | 0,4923 |
| 40 | -0,0005 | 0,0765 | 0,5232 |
| 50 | -0,0003 | 0,0726 | 0,5451 |
| 60 | -0,0002 | 0,0698 | 0,5623 |

Based on these data, the dependences of graphs $a = f(RS), b = f(RS), c = f(RS)$ are plotted, respectively Fig. 11-13.

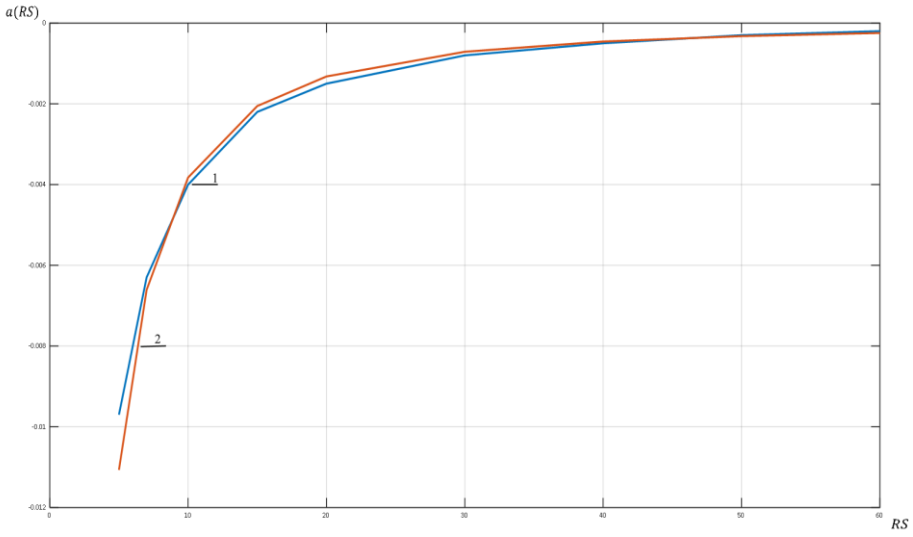


**Fig. 11.** Tabulated values (1) and approximating function $a = f(RS)$ (2) graphs

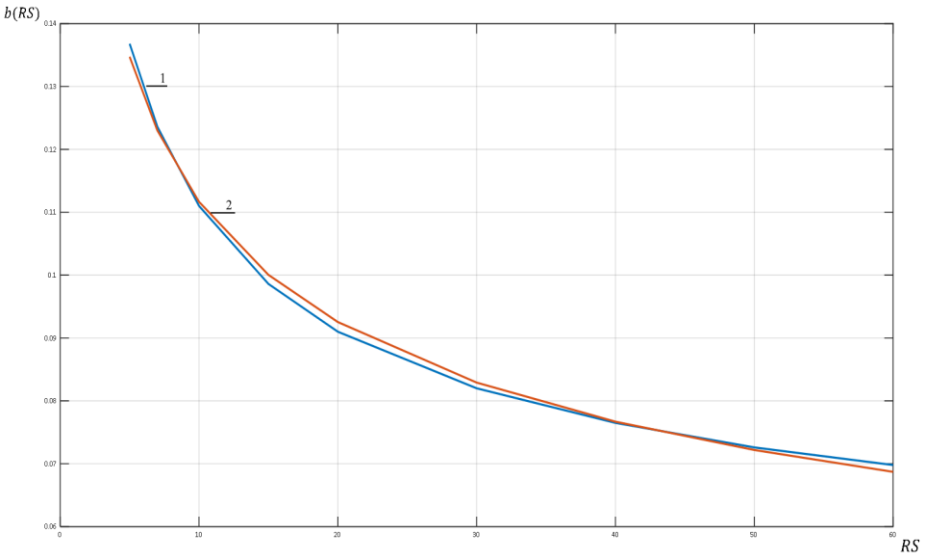


**Fig. 12.** Tabulated values (1) and approximating function $b = f\left(RS\right)$ (2) graphs

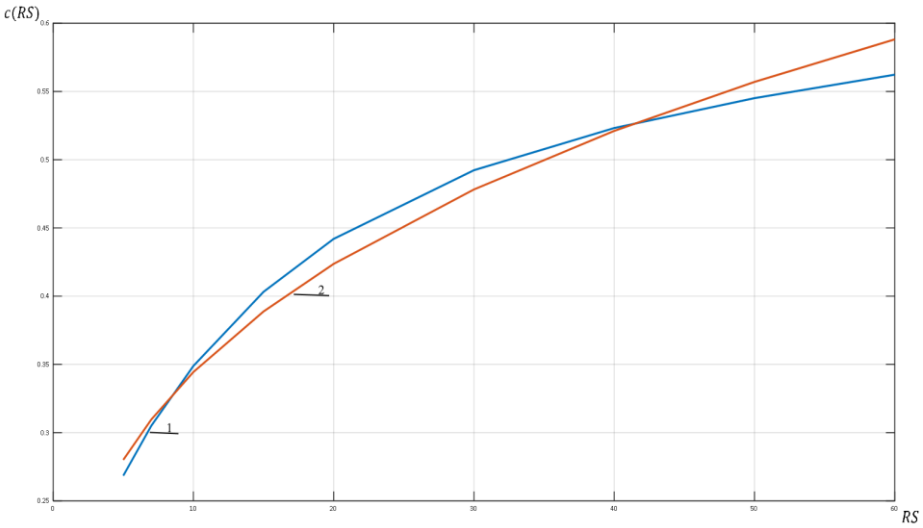


**Fig.13.** Tabulated values (1) and approximating function $c = f\left(RS\right)$ (2) graphs

The square error in each case was 0.016%, 0.038%, and 3.14%, respectively, and the approximating functions have the form

$$a = -0.1305038RS^{-1.533};$$
$$b = 0.2084RS^{-0.271};$$
$$c = 0.1732RS^{0.2986}.$$

Then, the phase value will be described by an approximating function

$$\varphi = -\pi\left[\left(-0.1305RS^{-1.533}\right)RP^2 + \left(0.2084RS^{-0.271}\right)RP + \left(0.1732RS^{0.2986}\right)\right]$$

## 3 Experimental verification

To verify experimentally the exposed theoretical provisions, we used an ultrasonic rangefinder, installed on the robotic system for assessing the distance to the obstacle. The rangefinder improved accuracy has been achieved by tuning the radiation frequency and, accordingly, rearrangement of channel for reflected signal processing. In the reflected signal processing path, we used a digital refrangible filter. Refer to Fig. 14 and 15 for details of filter operation.

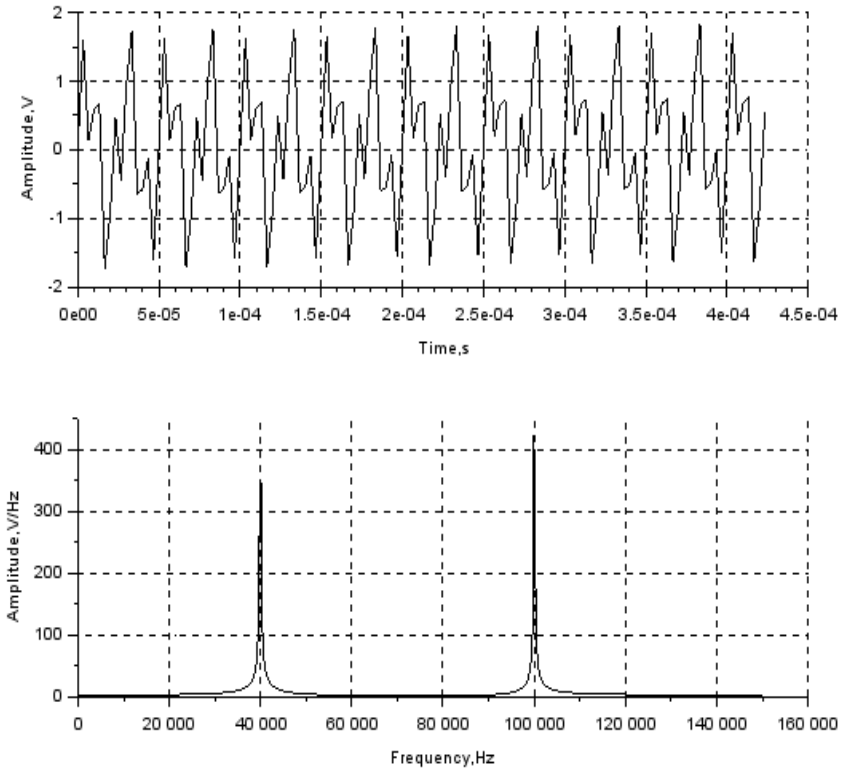


**Fig.14.** Filter input signal and signal spectrum

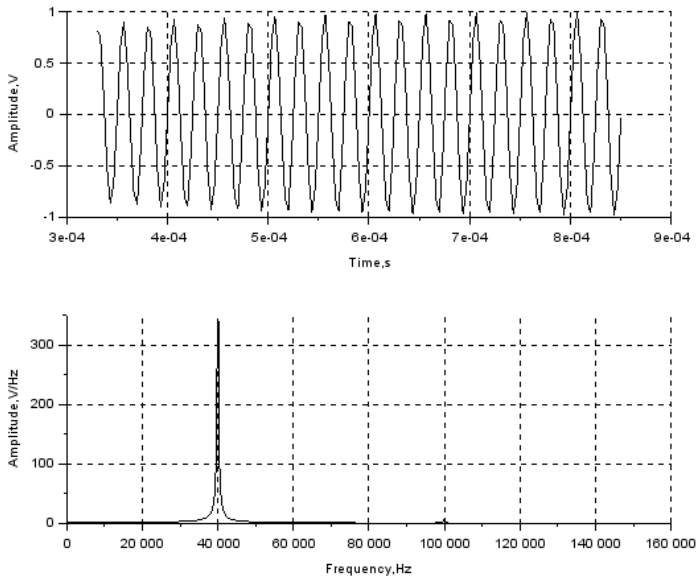


**Fig.15.** Filter output signal and signal spectrum

## 4 Conclusion

The obtained approximations of the PFR dependence on the ripple level and equations for finding the denominator coefficients of the digital filters transfer contributes to a more rapid using them in robotic systems. However, the resulting implementations are not quite simple. Therefore, expedient shall be continuing the search for a more convenient implementation on the microprocessor technology.

It should be borne in mind that the values of RP and RS do not change in large ranges. Usually they vary in narrow ranges and rarely. In this case, you can pre-calculate and use some pre-prepared values stored in memory. In the case of a sharp change in working conditions, these formulas can be useful for operational calculation, in order to maintain the best robotic system functioning.

## References

1. The Industry 4.0 Standards Landscape from a Semantic Integration Perspective Conference Paper (2018). https://www.researchgate.net/publication/318208930_The_Industry_40_Standards_Landscape_from_a_Semantic_Integration_Perspective

2. Industry 4.0: an overview. Conference Paper (2018). https://www.researchgate.net/publication/326352993_Industry_40_an_overview
3. Industry 4.0. https://www.cognex.com/ru-ru/what-is/industry-4-0-machine-vision/development.
4. Semenov S, Voloshyn D, Ahmed AN (2019) Mathematical model of the implementation process of flight task of unmanned aerial vehicle in the conditions of external impact. In: International Journal of Advanced Trends in Computer Science and Engineering, vol. 8(1), pp 7-13
5. Zhuravska I, Musyienko M, Tohoiev O (2019) Development the heat leak detection method for hidden thermal objects by means the information- measuring computer system. In: CEUR Workshop Proceedings, pp 350-364
6. Musiyenko MP, Denysov OO, Zhuravska IM, Burlachenko IS (2016) Development of double median filter for optical navigation problems. In: Proceedings of the 2016 IEEE 1st International Conference on Data Stream Mining and Processing, pp 177-181
7. Ukhina H, Sytnikov V, Streltsov O, Stupen P, Yakovlev D (2019) Transfer Function Coefficients Influence on the Processing Path Bandpass Frequency-Dependent Components' Amplitude-Frequency Characteristics Properties at the NPP TP ACS. In: Conference Proceedings of 2019 10th International Conference on Dependable Systems, Services and Technologies, DESSERT 2019, pp. 193-196. doi: 10.1109/DESSERT.2019.8770050
8. Eliseenko VV (2013) Information and control systems of NPPs produced by SNPO "Impulse". State, prospects, Jadernaja i radiatsionnaja bezopasnost, No 4(60), pp 61-64
9. Haridas N, Elias E (2016) Efficient variable bandwidth filters for digital hearing aid using farrow structure. Journal of Advanced Research, vol. 7(2), pp 255–262
10. Dhabu S, Ambede A (2018) Variable cutoff frequency fir filters: a survey. https://arxiv.org/ftp/arxiv/papers/1804/1804.02891.pdf
11. Koshita S, Abe M, Kawamata M (2018) Recent advances in variable digital filters. https://www.intechopen.com/books/digital-systems/recent-advances-in-variable-digital-filters
12. Ukhina HV, Afanasyev IV, Sytnikov VS (2019) The phase-frequency characteristic study of the second order digital frequency-dependent components of mobile platforms. In: Modern Information Tecnology 2019. Odesa: Ecology, pp 19-20.
13. Korn G, Korn T (1974) Mathematical Handbook for Scietists and Engineers. McGraw Hill Book Company, N.York, 832 p
14. Ukhina H, Sytnikov V, Streltsov O, Stupen P, Yakovlev D (2019) Stability evaluation based on the sustainability triangle application for transfer functions above 2nd order. In: CSAE 2019: Proceedings of the 3rd International Conference on Computer Science and Application Engineering, N. 6, pp 1–5 doi: https://doi.org/10.1145/3331453.3361305
15. Ukhina H, Sytnikov V, Streltsov O, Stupen P, Yakovlev D (2019) Specialized computer systems digital bandpass frequency-dependent components rearrangement. In: Proceedings of the 2019 10th IEEE International Conference on Intelligent Data Acquisition and Advanced Computing Systems: Technology and Applications, IDAACS. doi: 10.1109/IDAACS.2019.8924368
16. Zhengyou He. (2016) Wavelet Analysis and Transient Signal Processing Applications for Power Systems. Chine Electric Power Press, 252 p
17. Zahoor S, Naseem S (2017) Design and implementation of an efficient FIR digital filter. Electrical & electronic engineering | Research article, vol. 4, i. 1, pp 34-46.
18. Dzhigan VA (2013) Adaptive Signals Filtering: Theory and Algorithms. Tekhnosfera, 528 p